

Adsorption of Organic Matter from Papermaking Wastewater by CoFe₂O₄-Coated Sand in Batch and Fixed-Bed Systems

Lingyu Zeng,^a Yecan Peng,^{a,*} Guirong Ye,^{a,b} Xiaona Shang,^a Shuangfei Wang,^{a,b} and Jinghong Zhou^{a,*}

The secondary treated effluents of pulp and paper mills contain high chemical oxygen demand (COD) that is associated with organic matter. Therefore, this study explores the adsorption of substances contributing to COD using CoFe₂O₄ and quartz sand-coated CoFe₂O₄ in batch and fixed-bed column experiments. X-ray diffraction, scanning electron microscopy, Brunauer–Emmett–Teller analysis, and X-ray photoelectron spectroscopy were used to characterize the adsorbents. The quartz sand-loaded CoFe₂O₄ exhibited a larger pore volume and average pore size. Batch experiments revealed that adsorption on CoFe₂O₄ closely fit the pseudo-second-order model. To explore the effects of bed depth, feed flow rate, and initial solution pH on the breakthrough characteristics of CoFe₂O₄-coated sand, fixed-bed column experiments were conducted, and the breakthrough curves were drawn from the ratio of influent COD concentration to effluent COD concentration. The breakthrough time decreased with an increase in the feed flow rate and initial pH but increased with the bed depth. According to the X-ray photoelectron spectroscopy analysis, CoFe₂O₄-coated sand showed excellent stability due to negligible leaching of metallic elements. These findings have important implications for the advanced treatment of industrial wastewater.

Keywords: Fixed-bed column; CoFe₂O₄-coated sand; Adsorption; COD removal; Advanced treatment

Contact information: a: Guangxi Key Laboratory of Clean Pulp & Papermaking and Pollution Control, Light Industry and Food Engineering College, Guangxi University, Nanning 530004, China; b: Guangxi Bossco Environment Co., Ltd., Nanning 530007, China; *Corresponding author: jhzhoudou@gxu.edu.cn

INTRODUCTION

CoFe₂O₄ is a moderately saturated magnetic material with excellent chemical stability, mechanical hardness, and a wide optimum pH range (Zhang *et al.* 2017; Sohail *et al.* 2018). The introduction of Co to iron oxides has been reported to produce the compound Co_xFe_{3-x}O₄, which can promote both H₂O₂ decomposition and the oxidation of organic pollutants (Costa *et al.* 2006). Moreover, studies on the catalytic degradation of dye wastewater by CoFe₂O₄ nanoparticles have shown that CoFe₂O₄/GO exhibits superior catalytic activity for the removal of RhB (Dong *et al.* 2013). However, there are several drawbacks to the application of nano-sized ferrite particles. Aqueous CoFe₂O₄ nanoparticles are available in the form of a fine powder. In this form, CoFe₂O₄ has good adsorption performance for trace metals and organic pollutants; however, solid/liquid separation is difficult (Cheng *et al.* 2014). In addition, CoFe₂O₄ nanoparticles tend to aggregate and form large particles in aqueous solution, resulting in a loss of dispersion and specificity, reduced catalyst activity, and deteriorated adsorption performance. The immobilization of iron oxide nanoparticles on a quartz sand surface has been demonstrated

as a technique to preserve these unique catalyst properties (Yang *et al.* 2015). Iron oxide-coated sand is easy to prepare and convenient for use in filtration devices (Benjamin *et al.* 1996). Under these conditions, solid/liquid separation and regeneration are simple (Yang *et al.* 2015). Iron-coated sand has previously been used to remove organic contaminants and heavy metals from synthetic and real wastewater (Korshin *et al.* 1997; Lai and Chen 2001; Arias *et al.* 2006; Jiang *et al.* 2014; Liu *et al.* 2014). Vinosha *et al.* (2021) indicated that the application of CoFe_2O_4 in water treatment has not been sufficiently studied before and outlined the advantages of CoFe_2O_4 in water treatment. However, relatively few studies have been conducted on loading CoFe_2O_4 onto a sand surface and investigating its adsorption and degradation properties in real industrial wastewater. Loading CoFe_2O_4 onto the surface of quartz sand not only enables filtering and trapping but also increases the number of active adsorption sites on the surface of the quartz sand, which can then adsorb and remove dissolved pollutants in water. Moreover, quartz sand is easily separated from water and regenerated (Gao *et al.* 2020).

Pulp and paper (P&P) mills produce large amounts of wastewater with high suspended solids (SS), high color, and poor biodegradability (Toczyłowska-Maminska 2017). Secondary treatment technologies, such as primary clarification and biological treatment, are widely employed for papermaking wastewater treatment (Buyukkamaci and Koken 2010; Svensson and Berntsson 2014). However, conventional processes are not effective for the degradation of refractory organic pollutants; thus, secondary treated effluents still contain a considerable chemical oxygen demand (COD), toxicity, and color (Grötzner *et al.* 2018; Elnakar and Buchanan 2019). Many studies have shown that effluents from P&P mills seriously damage the environment (Ali and Sreekrishnan 2001; Sridhar *et al.* 2011; Wang *et al.* 2012b; Marques *et al.* 2017; Abedinzadeh *et al.* 2018). Under increasingly strict regulations for wastewater discharge, the search for efficient treatment techniques has become urgent.

In this study, CoFe_2O_4 was coated onto a sand surface and used to investigate the adsorption/desorption of organic pollutants from the secondary effluent of P&P mills *via* batch and column experiments. The prepared samples were characterized by X-ray diffraction (XRD), scanning electron microscopy (SEM), Brunauer-Emmett-Teller analysis (BET), and X-ray photoelectron spectroscopy (XPS). The main research topic, *i.e.*, the column adsorption of CoFe_2O_4 -coated sand, was analyzed through a detailed investigation of the experimental parameters and by establishing optimal experimental conditions.

EXPERIMENTAL

Materials

In this study, $\text{FeCl}_3 \cdot 6\text{H}_2\text{O}$, $\text{CoCl}_2 \cdot 6\text{H}_2\text{O}$, $\text{Al}(\text{NO}_3)_3 \cdot 9\text{H}_2\text{O}$, citric acid ($\text{C}_6\text{H}_8\text{O}_7 \cdot \text{H}_2\text{O}$), $\text{NH}_3 \cdot \text{H}_2\text{O}$ (25 to 28%), H_2O_2 (30%), p-chlorophenol, HCl, and NaOH were purchased from Aladdin Industrial Co., Ltd., Shanghai China. All chemical reagents were of analytical grade and used without further purification. Deionized water was used in all experiments. The wastewater used in the experiment was obtained from the bio-treated effluent of Guangxi Guitang Sugar Group Co., Ltd. (Guigang, China). The pH value of the wastewater was 7.00 ± 0.10 and the COD was 118.40 ± 0.10 mg/L.

CoFe₂O₄-coated Sand Preparation

A quartz sand size range of 0.6 to 0.8 mm was selected. The sand was pretreated in 0.1 mol/L HCl solution for 24 h, rinsed with deionized water, and dried at 105 ± 2 °C. A stock solution with a Co²⁺:Fe³⁺ molar ratio of 1:2 was prepared by dissolving CoCl₂ · 6H₂O (0.5 mol) and 1 mol FeCl₃ · 6H₂O in 40 mL of Milli-Q water. After 50 g of the pretreated quartz sand was added to the solution, the mixture was stirred well, and 20 mL of 0.8/L NaOH was added dropwise. After the reaction was complete, the composite was dried at 105 ± 2 °C for 12 h, transferred to a polytetrafluoroethylene autoclave, and reacted at 400 °C for 3 h. After cooling to room temperature (25 °C), the composite was washed with Milli-Q water to remove any CoFe₂O₄ particles that had failed to combine with the quartz sand. The scoured composition was then placed in a drying oven set at 105 ± 2 °C for 12 h, and the final CoFe₂O₄-coated sand composite was prepared.

Analytical Methods

CoFe₂O₄ and CoFe₂O₄-coated sand were analyzed using the following instruments or methods. The SEM was performed with a SU8220 instrument operating at 10 kV (Oxford spectroscopy; Hitachi, Tokyo, Japan). The XRD patterns were recorded using a MiniFlex 600 (Rigaku, Tokyo, Japan), with Cu-K α radiation, a voltage of 40 kV, and a scan range of 20 to 80° (2θ). The pore size and specific surface area were analyzed *via* N₂ adsorption and desorption with an American Mike (Micromeritics, Atlanta, GA, USA) ASAP 2460. The XPS was performed with a K-Alpha+ probe (Thermo Fisher Scientific, Waltham, MA, USA) using monochromatic Al-K α radiation ($h\nu = 1,486.6$ eV).

Batch Adsorption

Batch adsorption experiments were conducted at room temperature (25 °C). A certain amount of CoFe₂O₄-coated sand was placed in a 250-mL conical flask containing 50 mL of papermaking wastewater. The bottles were placed on a horizontal rotary shaker at 120 r/min for a certain period. Following the adsorption step, the liquid samples were filtered through a 0.45- μ m polycarbonate membrane, and the COD tests were conducted with the filtrate *via* potassium dichromate titration method. Each group of samples was analyzed in triplicate to obtain the average COD.

Tests Using a Mini-column

Column experiments were conducted in a glass column with an internal diameter of 7 cm and a length of 60 cm. In this experiment, three different sizes for the packed bed (10, 20, and 30 cm) were used, which corresponded to 150, 295, and 421 g of CoFe₂O₄-coated sand, respectively. The CoFe₂O₄-coated sand was loaded onto the column. A 5-cm high layer of quartz sand, with a diameter of 4 to 6 mm, was laid at the bottom of the column. Papermaking wastewater, with an initial COD concentration of 118.4 ± 0.10 mg/L, was pumped through the packed column at the desired flow rate using a peristaltic pump. Samples were collected from the column at regular time intervals and analyzed for their COD concentrations. Figure 1 shows the experimental setup. Samples were collected after adjusting the filter rate, and the COD was measured to determine the breakthrough curve of the adsorbed organic matter.

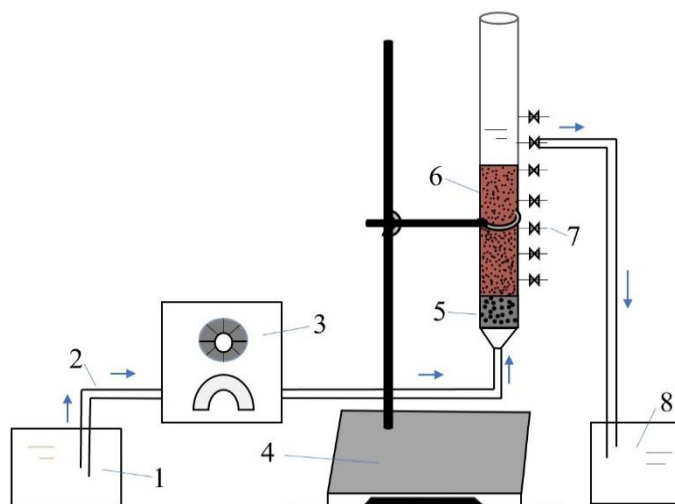


Fig. 1. Schematic of the experimental setup for the column studies (1: Wastewater; 2: Peristaltic pump hose; 3: Peristaltic pump; 4: Iron frame; 5: Retainer layer; 6: CoFe_2O_4 -coated sand; 7: Sampling hole; and 8: Adsorbed wastewater)

Regeneration

During the column adsorption tests, the adsorbed CoFe_2O_4 -coated sand was regenerated by running a 0.01/L NaOH solution in a constant-temperature water bath oscillator at 120 rpm and 303 K for 12 h. After washing to neutral, the regenerated CoFe_2O_4 -coated sand was reused to investigate its adsorption ability.

RESULTS AND DISCUSSION

Characterization of CoFe_2O_4 and CoFe_2O_4 -coated Sand

To explore the dispersion of CoFe_2O_4 particles on the sand surface, the morphology of the CoFe_2O_4 -coated sand was investigated *via* SEM (Fig. 2). The sand served as a support and was coated with well-dispersed CoFe_2O_4 . CoFe_2O_4 had a regular spherical or octahedral spinel structure with intergrouping of particles, which was consistent with the previously reported morphology of CoFe_2O_4 (Deng *et al.* 2013).

The XRD patterns were measured to investigate the crystal structure of CoFe_2O_4 , as shown in Fig. 3. CoFe_2O_4 exhibited seven diffraction peaks at $2\theta = 18.3^\circ$, 30.1° , 35.4° , 43.1° , 57.0° , 62.6° , and 74.0° , corresponding to the (111), (220), (311), (400), (511), (440), and (533) planes, respectively, which are characteristic XRD peaks of the cubic spinel structure of CoFe_2O_4 (Deng *et al.* 2013).

The elemental composition of the sand and CoFe_2O_4 -coated sand was examined *via* XPS (Fig. 4), which indicated three different peaks at 100, 285, and 530 eV, attributed to Si2p, C1s, and O1s, respectively. After CoFe_2O_4 was coated onto the sand surface, the peak intensities of Si and O decreased, and different peaks for Fe2p_{3/2} and Co2p_{3/2} appeared (Wang *et al.* 2012a), indicating that the Fe and Co compounds covered the sand surface. The atomic ratio of Fe/Co/O on the surface of the CoFe_2O_4 -coated sand was 23.58/10.94/45.68, which is similar to the stoichiometric ratio of CoFe_2O_4 . In summary, the results of the SEM, XRD, and XPS analyses showed that CoFe_2O_4 was successfully

deposited onto the surface of the quartz sand, changing the profile and modifying the surface chemical functional groups of the quartz sand.

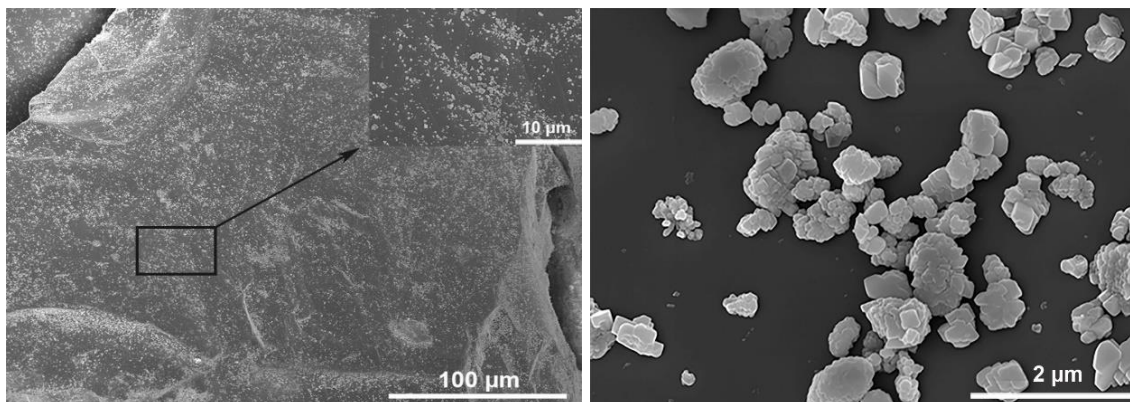


Fig. 2. SEM images of the CoFe₂O₄-coated sand

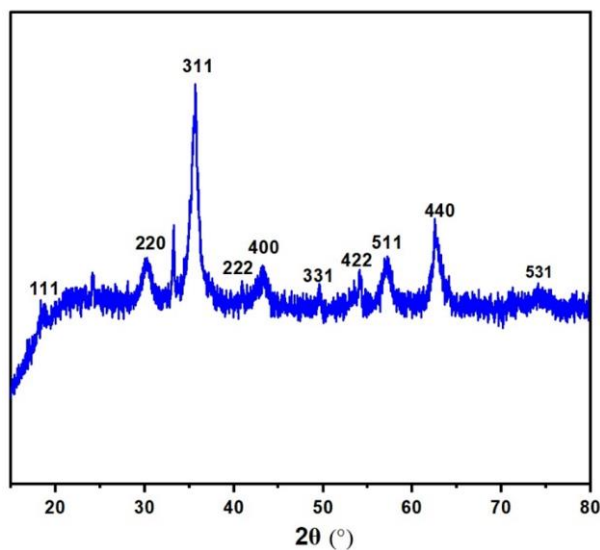


Fig. 3. XRD patterns of CoFe₂O₄

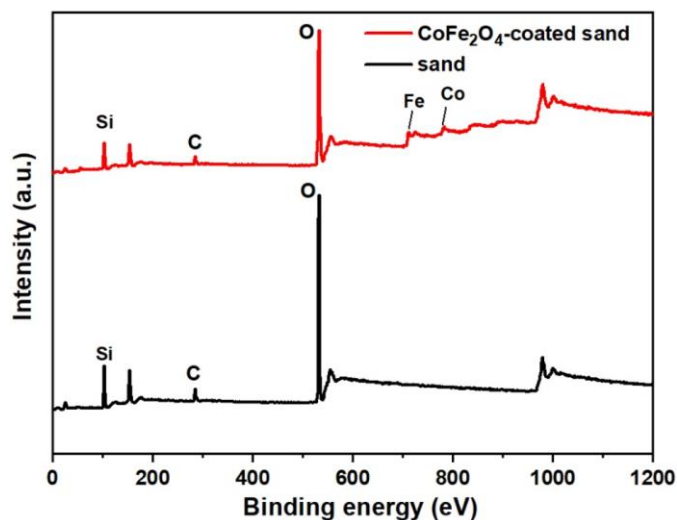


Fig. 4. XPS spectra of the sand (black line) and CoFe₂O₄-coated sand (red line)

The textural properties of the CoFe₂O₄ and CoFe₂O₄-coated sand were investigated using N₂ adsorption/desorption isotherms (Fig. 5a, b). Table 1 lists the BET specific surface area, pore volume, and mean pore diameter of CoFe₂O₄ and CoFe₂O₄-coated sand. CoFe₂O₄ exhibited a wide pore size distribution, with the pore diameter of CoFe₂O₄ nanocomposites ranging from 2.11 to 50.52 nm, whereas quartz sand loaded with CoFe₂O₄ exhibited a narrow pore size distribution of 1.7 to 29.8 nm, with a pore size distribution predominantly between 1.7 and 8.7 nm, indicating a mesoporous material (Fig. 5a, b). A hysteresis loop appeared at approximately $p/p_0 = 0.6$ in the adsorption-desorption isotherm of the CoFe₂O₄ and CoFe₂O₄-coated sand samples, indicating their porous structures. As listed in Table 1, the BET surface area of CoFe₂O₄-coated sand was 6.44 cm²/g, which was higher than that of the sand (0.1677 cm²/g). The CoFe₂O₄-coated quartz sand had a larger pore volume (0.00168 cm³/g) and average pore size (1.03 nm).

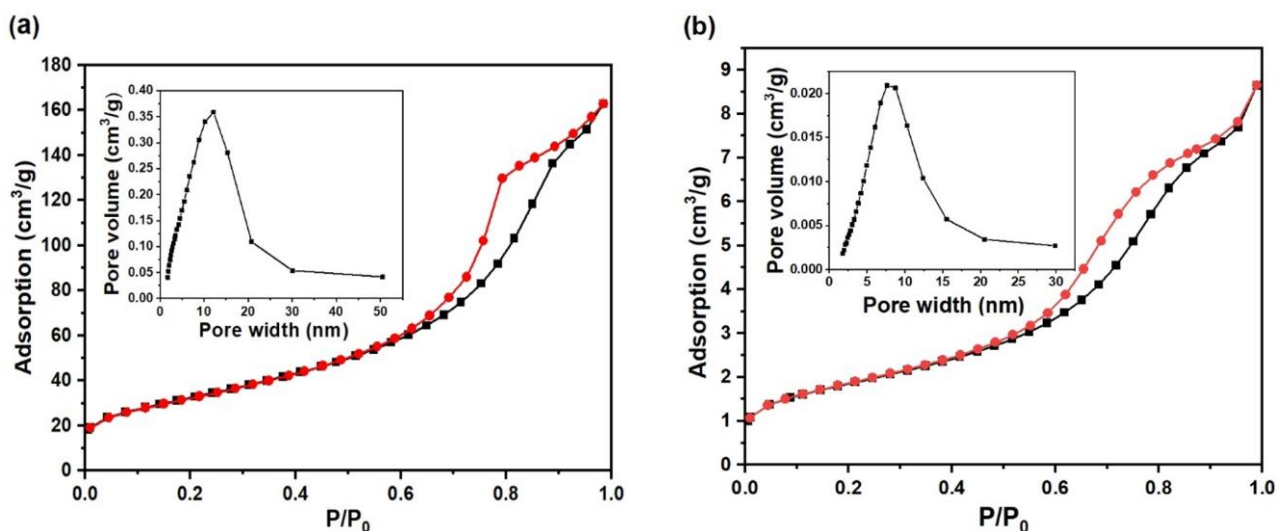


Fig. 5. N₂ adsorption-desorption isotherm and pore size distribution of (a) CoFe₂O₄ and (b) CoFe₂O₄-coated sand

Table 1. Specific Surface Area and Pore Size of the Sand and CoFe₂O₄-coated Sand

	Pore Volume (cm ³ /g)	Average Pore Size	Pore Volume (cm ³ /g)
Sand	0.00004	0.8333	0.1677
CoFe ₂ O ₄	0.02995	1.0579	114.47
CoFe ₂ O ₄ -coated Sand	0.00168	1.0321	6.4412

Batch Adsorption

In the batch experiments, the pH of the CoFe₂O₄ adsorption procedure ranged from 3 to 11 (Fig. 6). The pH values of the solutions were adjusted using 0.01 mol/L hydrochloric acid and sodium hydroxide. After the reaction, the solution was filtered through filter paper, and the COD tests were conducted with the filtrate *via* potassium dichromate titration method. The maximum removal rate of COD was 63.4% at a pH of 3 and the effluent COD was 40.2 mg/L. This indicated that the adsorption of COD was more favorable under acidic conditions. A similar result has been reported in which the collection rate of pectin continuously decreases when the pH increases from 2 to 5, which may be due to the decrease in the reducing ability of carboxyl groups under weak acid conditions (Nguyen *et al.* 2021). At pH values from 5 to 10, the COD removal rate decreased from 44.8 to 38.6% and exhibited a relatively stable trend, thereby broadening the range of pH applications of CoFe₂O₄ adsorbents. When the pH was increased to 11, the COD removal rate decreased to 26.0%. A study indicates that at basic pH, the adsorption rate decreases due to the formation of sulfate radicals that are quenched by OH⁻, while metal-hydroxide complexes may be formed on the surface of CoFe₂O₄ magnetic nanoparticles (MNPs), leading to a decrease in catalytic activity (Deng *et al.* 2013). In addition, the effect of pH on phenol in wastewater is significant, and the adsorption rate on phenol in wastewater dramatically decreased at pH above 8.5. Above this pH value, the phenol can be presented as phenolate ions (C₆H₅O⁻), thereby increasing the electrostatic repulsion with the carrier and leading to a decrease in adsorption capacity (Bouchra *et al.* 2019). These results indicate that the adsorption percentages for the organic pollutants strongly depend on the pH, and the adsorption capacity is large in the lower pH region.

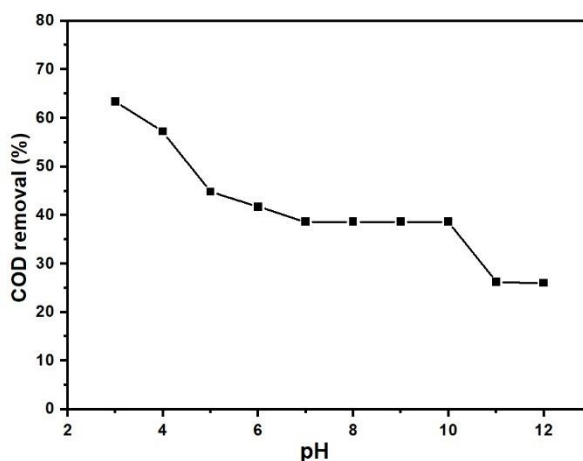


Fig. 6. Effect of pH on the removal efficiency of the COD (initial COD of 118.4 mg/L; CoFe_2O_4 of 0.15 g/50 mL; contact time of 2 h; and $T = 303\text{ K}$)

Figure 7 shows the contact time for the adsorption of COD onto CoFe_2O_4 at different COD concentrations. The adsorption equilibrium for COD on CoFe_2O_4 was less than 50 min. To better interpret the adsorption behavior of CoFe_2O_4 , pseudo-first-order (Eq. 1) and pseudo-second-order (Eq. 2) kinetic models were applied to fit the adsorption data:

$$q_t = q_e(1 - e^{-k_1 t}) \quad (1)$$

$$q_t = \frac{k_2 q_e^2 t}{1 + q_e k_2 t}, \quad (2)$$

where q_e and q_t (mg/g) are the adsorption capacities at equilibrium and time t , respectively, and k_1 and k_2 are the rate constants [g/(mg·min)]. As listed in Table 2, the pseudo-second-order kinetic model ($R^2 = 0.9857$) fit the experimental data better than the pseudo-first-order kinetic model ($R^2 = 0.8744$). The adsorption of organic pollutants on CoFe_2O_4 fit well with the pseudo-second-order model. In most cases, the pseudo-second-order model can be used to represent the relationship between time and the uptake of solutes in solution, and the adsorption mechanism is primarily governed by rates of diffusion. In the initial stage, the adsorption sites are sufficient, and therefore, the difference between the initial and final concentrations represents the largest and the most significant effect. However, as time progresses, the solutes in the solution are occupied after effective diffusion, resulting in only slight change in concentration (Hubbe *et al.* 2019). This was also reflected in the adsorption of dye wastewater, where a longer time was required for the dye molecules to reach the inside of the adsorbent to achieve maximum adsorption efficiency on the adsorbate (Hubbe *et al.* 2012).

Table 2. Kinetic Model Parameters for the Adsorption of COD by CoFe_2O_4

Models	Parameters			
	Q_e	K_1	K_2	R^2
Pseudo-first-order	17.29	1.07		0.8744
Pseudo-second-order	17.29		0.058	0.9857

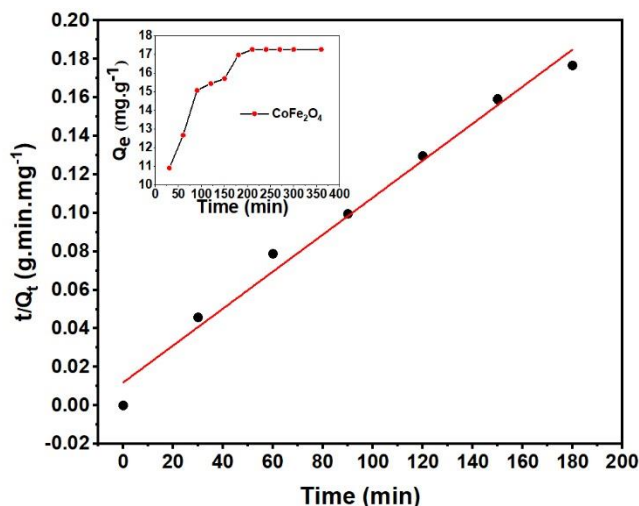


Fig. 7. Effect of the contact time on the removal efficiency of the COD and corresponding pseudo-second order kinetics plots

Adsorption in Fixed-bed Column Reactor

The breakthrough curves for the column were calculated by plotting the ratio of C_e/C_0 (C_e is the effluent COD concentration and C_0 is the influent COD concentration) against time. In the removal of Cu^{2+} using raw rice hulls (RRH) and expanding rice husk (ERH), the breakthrough concentration is typically set to 10% of the initial concentration (C_0) (Luo *et al.* 2011). The wastewater treated in this study was obtained from a papermaking mill, and the water pollutant discharge standard of the China papermaking industry for discharging papermaking wastewater after treatment is 50 mg/L as per GB 3544 (2008). Therefore, in this study, the breakthrough concentration (C_b) was set to 50 mg/L ($C_b/C_0 = 0.42$).

To confirm the role of the CoFe_2O_4 -coated sand in COD removal, the authors used raw sand as the blank control for the column adsorption test. The parameters were as follows: bed depth = 20 cm, COD = 118 mg/L, and flow rate = 3.5 mg/min. According to Fig. 8(a), raw sand had a negligible effect on COD removal. In the adsorption process, pollutants must have sufficient time to diffuse into the adsorbent. When the flow rate was too high, the adsorption did not reach equilibrium and the saturated extent of adsorption was small; when the flow rate was too low, the adsorption efficiency was improved, but the capacity of the reactor was reduced. Therefore, the influent flow rate is an important index for the adsorption column. The adsorption column experiment was conducted at different flow rates (3.5, 4.5, and 5 mg/min), the initial COD concentration was 118.4 mg/L, and the bed depth was 20 cm. As shown in Fig. 8(b), the breakthrough time varied with the flow rate. As the flow rate increased from 3.5 to 5 mg/min, the breakthrough time decreased from 20 to 5 min. An increase in the flow rate reduced the contact time between the pollutants and the bed, resulting in a decrease in the treatment efficiency prior to the breakthrough point. Therefore, an increase in the empty bed contact time will slowly increase the penetration curve and increase water production. This may be because the loaded CoFe_2O_4 increased the specific surface area of the adsorbent, which led to an increase in the number of adsorption sites.

The bed depths of the column adsorption experiments were 10, 20, and 30 cm, corresponding to 150, 295, and 421 g of CoFe_2O_4 -coated sand, respectively. Figure 8(c) shows the effect that the bed depth has on the shape of the breakthrough curves. The breakthrough time increased with an increase in the bed depth. When the bed depth of the packed bed decreased, the mass transfer process of pollutants was predominantly axial dispersion, and the pollutants did not have sufficient time to diffuse into the entire adsorbent, thus reducing the diffusion of the pollutants (Baral *et al.* 2009; Chen *et al.* 2011). In addition, an increase in the bed depth increased the specific surface area of CoFe_2O_4 -coated sand from that of raw sand, which provided more fixed binding sites for the pollutants, resulting in an increased residence time of the pollutants in the bed. Therefore, an increase in the height of the packing layer causes the breakthrough point of the adsorption curve to move in the direction of an increased volume of treated solution.

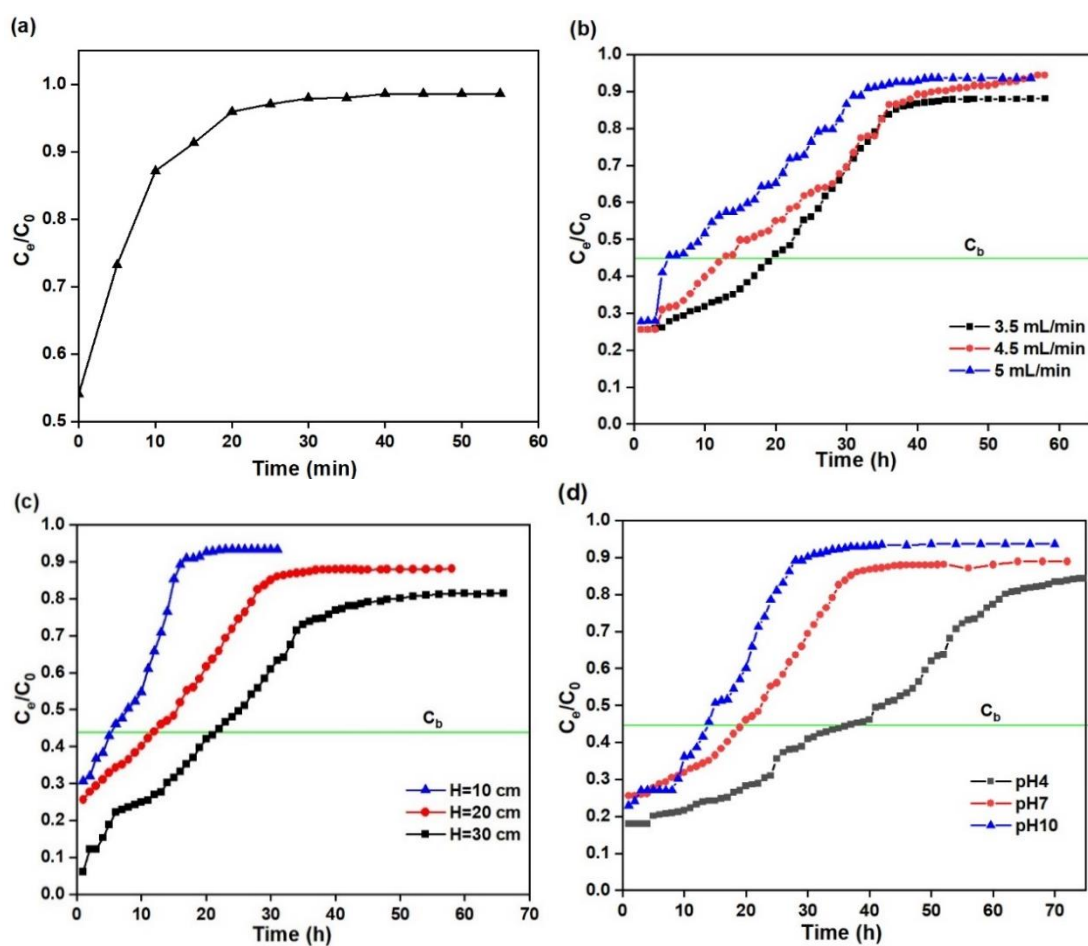


Fig. 8. (a) Breakthrough curve for raw sand (blank control) (bed depth = 20 cm; COD = 118.4 mg/L; pH = 7.0 ± 0.1 ; and $u = 3.5$ mg/min). (b) Breakthrough curves of COD removal for CoFe_2O_4 -coated sand at different flow rates (bed depth = 20 cm; COD = 118.4 mg/L; and pH = 7.0 ± 0.1). (c) Breakthrough curves of COD removal for CoFe_2O_4 -coated sand at different bed depths (COD = 118.4 mg/L; pH = 7.0 ± 0.1 ; and $u = 3.5$ mg/min). (d) Breakthrough curves of COD removal for CoFe_2O_4 -coated sand at different pH values (bed depth = 20 cm; COD = 118.4 mg/L; and $u = 3.5$ mg/min)

Figure 8(d) shows the breakthrough curves obtained at pH values of 4, 7, and 10. The longest breakthrough time was obtained at a pH of 4. The breakthrough times were 14, 19, and 37 h for pH values of 10, 7, and 4, respectively.

These results indicate that the adsorption capacity of organic pollutants in CoFe₂O₄-coated sand was remarkably greater than that in raw sand. Thus, CoFe₂O₄-coated sand, as an effective filter material, has good application prospects for the advanced treatment of real industrial wastewater.

Stability and Reusability

Reusability is one of the most important considerations in the applicability of adsorbents. In this study, CoFe₂O₄-coated sand was collected after adsorption and soaked in 0.01/L NaOH for 24 h, washed several times with water to obtain a neutral pH, and reused for COD adsorption. As shown in Fig. 9, the CoFe₂O₄-coated sand exhibited a promising reusability performance.

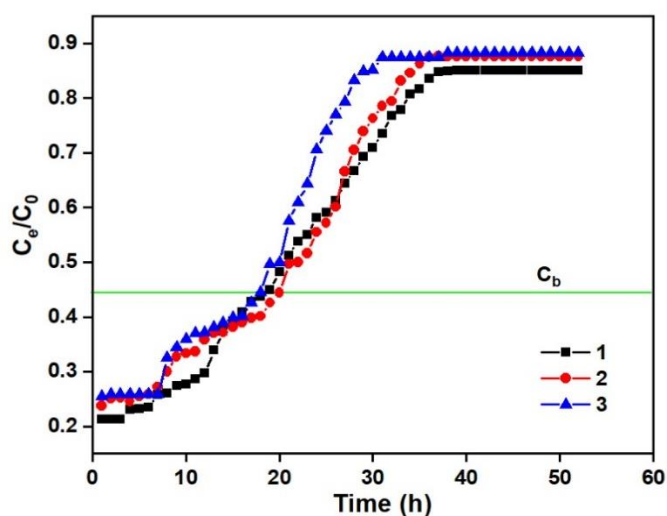


Fig. 9. Breakthrough curves of the regenerated CoFe₂O₄-coated sand ($C_0 = 118.4$ mg/L; bed depth = 20 cm; $u = 3.5$ mg/min; $pH = 7.0 \pm 0.1$; and reused for three cycles)

The breakthrough times were 20, 19, and 18 h for the first, second, and third reuses, respectively. These experiments indicate that the adsorption capacity decreased slightly after successive reuses. Furthermore, the fresh and used CoFe₂O₄-coated sand after degradation were analyzed *via* XPS. According to the full-scale XPS spectrum (Fig. 10), there was no notable difference between the fresh and used sand, indicating that no chemical or structural changes occurred in the adsorbent. The high resolution of Fe2p was deconvoluted into three spectral bands at 710.1, 712.7, and 723.9 eV for CoFe₂O₄-coated sand before and after use (Wang *et al.* 2012a; Wan and Wang 2017). Based on the Fe2p envelope, Fe³⁺ and Fe²⁺ accounted for 74.4 and 25.6% of the fresh CoFe₂O₄-coated sand, respectively, and Fe³⁺ and Fe²⁺ accounted for 71.1 and 28.9% of the used CoFe₂O₄-coated sand, respectively. The peak Co2p3/2 occurred at 779.8, 781.9, and 785.9 eV (Ren *et al.* 2015), where Co²⁺ and Co³⁺ accounted for 29 and 71% of the fresh CoFe₂O₄-coated sand, respectively, and Co²⁺ and Co³⁺ accounted for 28.5 and 71.5% after treatment, respectively. The results exhibited no notable difference between the fresh and used CoFe₂O₄-coated sand, indicating that CoFe₂O₄-coated sand has excellent stability.

The high resolution of C1s exhibited three main peaks at 284.8, 286.0, and 288.4 eV, corresponding to C–C/C=C, C–O–C/C–OH, and C=O, respectively (Fig. 10d) (Janos *et al.* 2017). The results showed that the contents of C–O and C=O increased from 27.70 and 8.59% to 32.10 and 10.90%, respectively. This indicates that organic matter was chemisorbed on the surface of the CoFe₂O₄-coated sand (Sreeprasad *et al.* 2011).

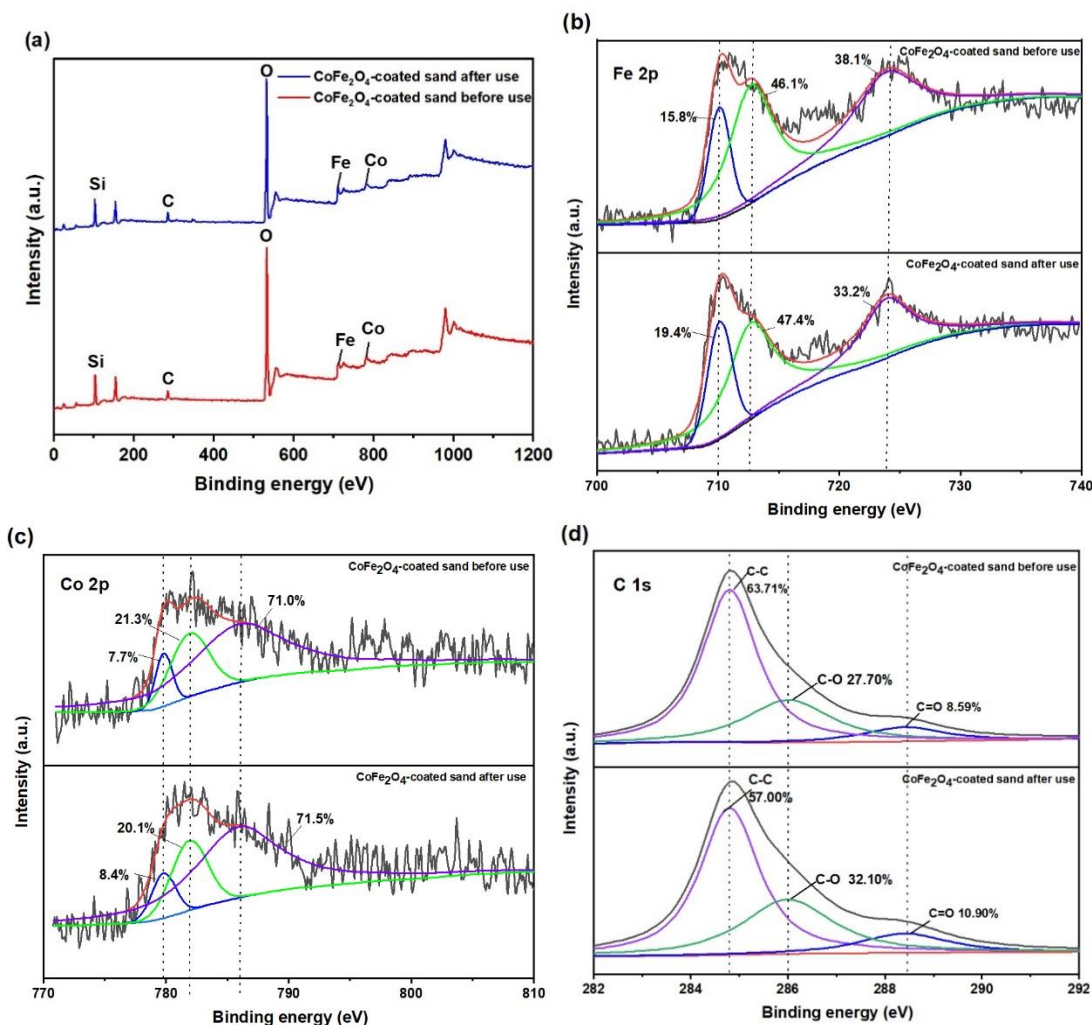


Fig. 10. (a) Wide-scale XPS spectra of CoFe₂O₄-coated sand before and after adsorption. (b) XPS spectra of Fe^{2p} in the CoFe₂O₄-coated sand before and after adsorption. (c) XPS spectra of Co_{2p} in the CoFe₂O₄-coated sand before and after adsorption. (d) XPS spectra of C1s in the CoFe₂O₄-coated sand before and after adsorption

CONCLUSIONS

1. CoFe₂O₄-coated sand can be effectively used as an adsorbent for the adsorption of COD-contributing organic substances present in paper wastewater owing to its advantages such as significant increase in specific surface area and easy recovery.
2. The results of fixed-bed column experiments showed that the qualified water yield required to reach the breakthrough concentration was directly proportional to the height

of the adsorption bed and inlet flow rate. Moreover, column adsorption was more efficient under acidic conditions.

3. The regeneration experiment using the adsorption column showed that the qualified water volume was similar after three regeneration cycles, which indicated that the CoFe₂O₄-coated sand adsorption column can be reused and has a good regeneration capacity for the adsorption of chemical oxygen demand (COD).
4. The findings support the conclusion that the CoFe₂O₄-coated sand-based adsorption process is promising for the advanced treatment of industrial wastewater.

ACKNOWLEDGMENTS

This study was financially supported by the Guangxi Open Fund for Clean Pulp and Paper and Pollution Control, Guangxi University (ZR201801-7). The authors also thank the Guangxi Sugar Industry Collaborative Innovation Center for assistance with the laboratory instruments.

REFERENCES CITED

- Abedinzadeh, N., Shariat, M., Monavari, S. M., and Pendashteh, A. (2018). "Evaluation of color and COD removal by Fenton from biologically (SBR) pre-treated pulp and paper wastewater," *Process Saf. Environ. Prot.* 116, 82-91. DOI: 10.1016/j.psep.2018.01.015
- Ali, M., and Sreekrishnan, T. R. (2001). "Aquatic toxicity from pulp and paper mill effluents: A review," *Adv. Environ. Res.* 5(2), 175-196. DOI: 10.1016/S1093-0191(00)00055-1
- Arias, M., Silva-Carballal, J. D., García-Río, L., Mejuto, J., and Nunez, A. (2006). "Retention of phosphorus by iron and aluminum-oxides-coated quartz particles," *J. Colloid Interface Sci.* 295(1), 65-70. DOI: 10.1016/j.jcis.2005.08.001
- Baral, S. S., Das, N., Ramulu, T. S., Sahoo, S. K., Das, S. N., and Chaudhury, G. R. (2009). "Removal of Cr(VI) by thermally activated weed *Salvinia cucullata* in a fixed-bed column," *J. Hazard Mater.* 161(2-3), 1427-1435. DOI: 10.1016/j.jhazmat.2008.04.127
- Bouchra, B. M., Khalid, Y., Najib, T., Awad, A. A., Hafid, Z., Younes, D., Ill-Min, C., Seung-Hyun, K., and Hassane, L. (2019). "Adsorptive removal of phenol using faujasite-type Y zeolite: Adsorption isotherms, kinetics and grand canonical Monte Carlo simulation studies." *J. Mol. Liq.* 296(15), article no. 111997. DOI: 10.1016/j.molliq.2019.111997
- Benjamin, M. M., Sletten, R. S., Bailey, R. P., and Bennett, T. (1996). "Sorption and filtration of metals using iron-oxide-coated sand," *Water Res.* 30(11), 2609-2620. DOI: 10.1016/S0043-1354(96)00161-3
- Buyukkamaci, N., and Koken, E. (2010). "Economic evaluation of alternative wastewater treatment plant options for pulp and paper industry," *Sci. Total Environ.* 408(24), 6070-6078. DOI: 10.1016/j.scitotenv.2010.08.045

- Chen, N., Zhang, Z., Feng, C., Li, M., Chen, R., and Sugiura, N. (2011). "Investigations on the batch and fixed-bed column performance of fluoride adsorption by Kanuma mud," *Desalination* 268(1-3), 76-82. DOI: 10.1016/j.desal.2010.09.053
- Cheng, T., Zhang, D., Li, H., and Liu, G. (2014). "Magnetically recoverable nanoparticles as efficient catalysts for organic transformations in aqueous medium," *Green Chem.* 16(7), 3401-3427. DOI: 10.1039/c4gc00458b
- Costa, R. C. C., Lelis, M. F. F., Oliveira, L. C. A., Fabris, J. D., Ardisson, J. D., Rios, R. R. V. A., Silva, C. N., and Lago, R. M. (2006). "Novel active heterogeneous Fenton system based on $\text{Fe}_{3-x}\text{M}_x\text{O}_4$ (Fe, Co, Mn, Ni): The role of M^{2+} species on the reactivity towards H_2O_2 reactions," *J. Hazard Mater.* 129(1-3), 171-178. DOI: 10.1016/j.jhazmat.2005.08.028
- Deng, J., Shao, Y., Gao, N., Tan, C., Zhou, S., and Hu, X. (2013). "CoFe₂O₄ magnetic nanoparticles as a highly active heterogeneous catalyst of oxone for the degradation of diclofenac in water," *J. Hazard Mater.* DOI: 10.1016/j.jhazmat.2013.09.049
- Dong, M., Lin, Q., Chen, D., Fu, X., Wang, M., Wu, Q., Chen, X., and Li, S. (2013). "Amino acid-assisted synthesis of superparamagnetic CoFe₂O₄ nanostructures for the selective adsorption of organic dyes," *RSC Adv.* 3(29), 11628-11633. DOI: 10.1039/c3ra40469b
- Elnakar, H., and Buchanan, I. D. (2019). "Pulp and paper mill effluent management," *Water Environ. Res.* 91(10), 1069-1071. DOI: 10.2175/106143018X15289915807164
- Gao, D., Junaid, M., Lin, F., Zhang, S., and Xu, N. (2020). "Degradation of sulphachloropyridazine sodium in column reactor packed with CoFe₂O₄ loaded quartz sand via peroxymonosulfate activation: Insights into the amorphous phase, efficiency, and mechanism," *Chem. Eng. J.* 390, Article ID 124549. DOI: 10.1016/j.cej.2020.124549
- GB 3544 (2008). "Discharge standard for industrial water pollution of pulp and paper industry," Standardization Administration of China, Beijing, China.
- Grötzner, M., Melchior, E., Schroeder, L. H., Dos Santos, A. R., Moscon, K. G., De Andrade, M. A., Martinelli, S. H. S., and Xavier, C. R. (2018). "Pulp and paper mill effluent treated by combining coagulation-flocculation-sedimentation and Fenton processes," *Water Air Soil Pollut.* 229(11), 1-7. DOI: 10.1007/s11270-018-4017-5
- Hubbe, M. A., Azizian, S., and Douven, S. (2019). "Implications of apparent pseudo-second-order adsorption kinetics onto cellulosic materials. A review," *BioResources* 14(3), 7582-7626. DOI: 10.15376/biores.14.3.7582-7626
- Hubbe, M. A., Beck, K. R., O'Neal, W. G., and Sharma, Y. C. (2012). "Cellulosic substrates for removal of pollutants from aqueous systems: A review. 2. Dyes," *Bioresources* 7(2), 2592-2687. DOI: 10.15376/biores.7.2.2592-2687
- Janos, P., Tolasz, J., Ederer, P. G., Ognen, E., and Petra, B. (2017). "Determination of amino groups on functionalized graphene oxide for polyurethane nanomaterials: XPS quantitation vs. functional speciation," *RSC Adv.* 7(21), 12464-12473. DOI: 10.1039/c6ra28745j
- Jiang, C., Jia, L., Zhang, B., He, Y., and Kirumba, G. (2014). "Comparison of quartz sand, anthracite, shale and biological ceramsite for adsorptive removal of phosphorus from aqueous solution," *J. Environ. Sci.* 26(2), 466-477. DOI: 10.1016/S1001-0742(13)60410-6
- Korshin, G. V., Benjamin, M. M., and Sletten, R. S. (1997). "Adsorption of natural organic matter (NOM) on iron oxide: Effects on NOM composition and formation of

- organo-halide compounds during chlorination," *Water Res.* 31(7), 1643-1650. DOI: 10.1016/S0043-1354(97)00007-9
- Lai, C. H., and Chen, C. Y. (2001). "Removal of metal ions and humic acid from water by iron-coated filter media," *Chemosphere* 44(5), 1177-1184. DOI: 10.1016/S0045-6535(00)00307-6
- Liu, J., Li, J., Mei, R., Wang, F., and Sellamuthu, B. (2014). "Treatment of recalcitrant organic silicone wastewater by fluidized-bed Fenton process," *Sep. Purif. Technol.* 132, 16–22. DOI: 10.1016/j.seppur.2014.04.050
- Luo, X., Deng, Z., Lin, X., and Zhang, C. (2011). "Fixed-bed column study for Cu²⁺ removal from solution using expanding rice husk," *J. Hazard Mater.* 187(1-3), 182-189. DOI: 10.1016/j.jhazmat.2011.01.019
- Marques, R. G., Ferrari-Lima, A. M., Slusarski-Santana, V., and Fernandes-Machado, N. R. C. (2017). "Ag₂O and Fe₂O₃ modified oxides on the photocatalytic treatment of pulp and paper wastewater," *J. Environ. Manage.* 195(Part 2), 242-248. DOI: 10.1016/j.jenvman.2016.08.034
- Nguyen, L. H., Van, H. T., Quan, D. H., and Pham, P. T. T. (2021). "Magnetic nanocomposite derived from nopal cactus biopolymer and magnetic nanoparticles used for the microalgae flocculation of aqueous solution," *BioResources.* 16(2), 3469-3493. DOI: 10.15376/biores.16.2.3469-3493
- Ren, Y., Lin, L., Ma, J., Yang, J., Feng, J., and Fan, Z. (2015). "Sulfate radicals induced from peroxymonosulfate by magnetic ferrosin MF₂O₄ (M = Co, Cu, Mn, and Zn) as heterogeneous catalysts in the water," *Appl. Catal. B- Environ.* 165, 572-578. DOI: 10.1016/j.apcatb.2014.10.051
- Sohail, M., Xue, H., Jiao, Q., Hansheng, K., and Khakemin, W. (2018). "Synthesis of well-dispersed TiO₂/CNTs@CoFe₂O₄ nanocomposites and their photocatalytic properties," *Mater. Res. Bull.* 101(5), 83-89. DOI: 10.1016/j.materresbull.2018.01.017
- Sreepasad, T. S., Maliyekkal, S. M., Lisha, K. P., and Pradeep, T. (2011). "Reduced graphene oxide–metal/metal oxide composites: Facile synthesis and application in water purification," *J. Hazard Mater.* 186(1), 921-931. DOI: 10.1016/j.jhazmat.2010.11.100
- Sridhar, R., Sivakumar, V., Immanuel, V. P., and Maran, J. P. (2011). "Treatment of pulp and paper industry bleaching effluent by electrocoagulant process," *J. Hazard Mater.* 186(2-3), 1495-1502. DOI: 10.1016/j.jhazmat.2010.12.028
- Svensson, E., and Berntsson, T. (2014). "The effect of long lead times for planning of energy efficiency and biorefinery technologies at a pulp mill," *Renew. Energy* 61(1), 12-16. DOI: 10.1016/j.renene.2012.04.029
- Toczyłowska-Maminska, R. (2017). "Limits and perspectives of pulp and paper industry wastewater treatment – A review," *Renew. Sust. Energy Rev.* 78(10), 764-772. DOI: 10.1016/j.rser.2017.05.021.
- Vinoshia, P. A., Manikandan, A., Preetha, A. C., Dinesh, A., Slimani, Y., Almessiere, M. A., Baykal, A., Xavier, B., and Nirmala, G. F. (2021). "Review on recent advances of synthesis, magnetic properties, and water treatment applications of cobalt ferrite nanoparticles and nanocomposites," *J. Supercond. Nov. Magn.* 34, 995-1018. DOI: 10.1007/s10948-021-05854-6
- Wan, Z., and Wang, J. (2017). "Degradation of sulfamethazine using Fe₃O₄-Mn₃O₄/reduced graphene oxide hybrid as Fenton-like catalyst," *J. Hazard Mater.* 324, 653-664. DOI: 10.1016/j.jhazmat.2016.11.039.

- Wang, W. P., Yang, H., Xian, T., and Jiang, J. L. (2012a). "XPS and magnetic properties of CoFe₂O₄ nanoparticles synthesized by a polyacrylamide gel route," *Mater. Trans.* 53(9), 1586-1589. DOI: 10.2320/matertrans.M2012151
- Wang, X., Liu, J., Ren, N. Q., and Duan, Z. (2012b). "Environmental profile of typical anaerobic/anoxic/oxic wastewater treatment systems meeting increasingly stringent treatment standards from a life cycle perspective," *Bioresource Technol.* 126, 31-40. DOI: 10.1016/j.biortech.2012.09.009
- Yang, X., Shi, Z., and Liu, L. (2015). "Adsorption of Sb(III) from aqueous solution by QFGO particles in batch and fixed-bed systems," *Chem. Eng. J.* 260(15), 444-453. DOI: 10.1016/j.cej.2014.09.036
- Zhang, S., Qi, Z., Zhao, Y., Jiao, Q., Ni, X., Wang, Y., Chang, Y., and Ding, C. (2017). "Core/shell structured composites of hollow spherical CoFe₂O₄ and CNTs as absorbing materials," *J. Alloys Com.* 694, 309-312. DOI: 10.1016/j.jallcom.2016.09.324

Article submitted: February 19, 2021; Peer review completed: June 13, 2021; Revised version received and accepted: June 25, 2021; Published: July 2, 2021.
DOI: 10.15376/biores.16.3.5806-5820